NANO LETTERS

Letter

pubs.acs.org/NanoLett

# Integrated Diamond Networks for Quantum Nanophotonics

Birgit J. M. Hausmann,[†] Brendan Shields,[‡] Qimin Quan,[†] Patrick Maletinsky,[‡] Murray McCutcheon,[†] Jennifer T. Choy,[†] Tom M. Babinec,[†] Alexander Kubanek,[‡] Amir Yacoby,[‡] Mikhail D. Lukin,[‡] and Marko Lončar*,[†]

[†]School of Engineering and Applied Sciences, Harvard University, 33 Oxford Street, Cambridge, Massachussetts, United States

[‡]Department of Physics, Harvard University, 17 Oxford Street, Cambridge, Massachussetts, United States

Supporting Information

**ABSTRACT:** We demonstrate an integrated nanophotonic network in diamond, consisting of a ring resonator coupled to an optical waveguide with grating in- and outcouplers. Using a nitrogen-vacancy color center embedded inside the ring resonator as a source of photons, single photon generation and routing at room temperature is observed. Furthermore, we observe a large overall photon extraction efficiency (10%) and high quality factors of ring resonators (3200 for waveguide-coupled system and 12 600 for a bare ring).

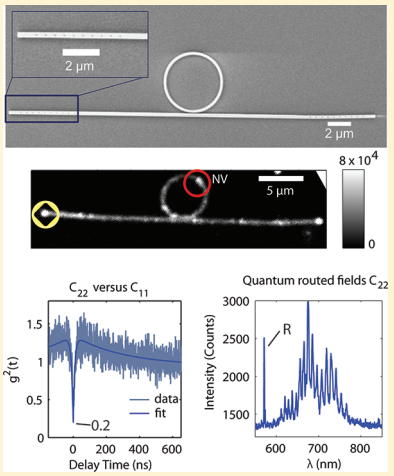


**KEYWORDS:** *Nitrogen-vacancy (NV) center, diamond, photonic crystal cavity, single photon source, cavity QED, on-chip photonics*



For applications in quantum information science and technology, diamond offers unique advantages over other solid-state platforms. The existence of luminescent defects such as nitrogen vacancy (NV) centers that can be used as a long-lived (spin-based) memory with optical read-out, makes diamond a promising platform for quantum information processing (QIP).[1−3] In particular, NV centers coupled to a resonator could form a quantum node of a quantum network to store, manipulate, and process information while waveguides could represent quantum channels between the nodes that transfer quantum information.[3,4] While proof-of-principle quantum networks with diamond NV centers have previously been demonstrated,[5,6] the scalability of the approach crucially depends on the realization of an integrated diamond nanophotonic platform. Until recently scalable diamond photonics has been limited to bulk[7−12] or polycrystalline diamond devices[13−15] due to difficulties associated with the fabrication of thin, single crystal, diamond (SCD) films on sacrificial or low index substrates. Light absorption and scattering at grain boundaries can be detrimental for the polycrystalline diamond approaches, while the realization of scalable, on-chip quantum networks is challenging with single-crystal bulk diamond approaches. Here, we demonstrate the building block of an all-diamond photonic network on chip that overcomes these issues and represents a leap forward for quantum optics applications. The node of the network consists of a single NV center coupled to the mode of a high-Q ring resonator and a low loss waveguide that is evanescently coupled to the cavity could be used as a routing element between nodes.

Our approach involves the fabrication of high quality, low loss ring resonators directly in single crystal diamond (SCD) thin slabs. Figure 1a illustrates our fabrication sequence, based on the approach that we[16,17] as well as others[18] have recently demonstrated. First we thin a 20 $\mu$m thick type Ib single crystal diamond slab (Element Six) to the preferred device layer thickness by an oxygen-based inductively coupled reactive ion etch (ICP RIE).[19] An e-beam (Elionix) exposes XR e-beam resist (spin-on-glass, Dow Corning) to form a mask that we transfer to the diamond film in a second etch. Figure 1b shows a scanning electron microscope (SEM) image of representative diamond ring resonators with different diameter and ring cross-sectional dimensions on $SiO_2$/Si substrate.

In order to characterize our diamond resonators, we take advantage of the intrinsic fluorescence of embedded color centers. We use a photoluminescence approach in a scanning confocal microscope using two collection arms[20] (Figure 1 and Supporting Information). Green pump light (532 nm) scans the devices at normal incidence (Figure 1c) via a scanning

**Received:** December 16, 2011
**Revised:** February 7, 2012
**Published:** February 16, 2012

   dx.doi.org/10.1021/nl204449n | *Nano Lett.* 2012, 12, 1578−1582

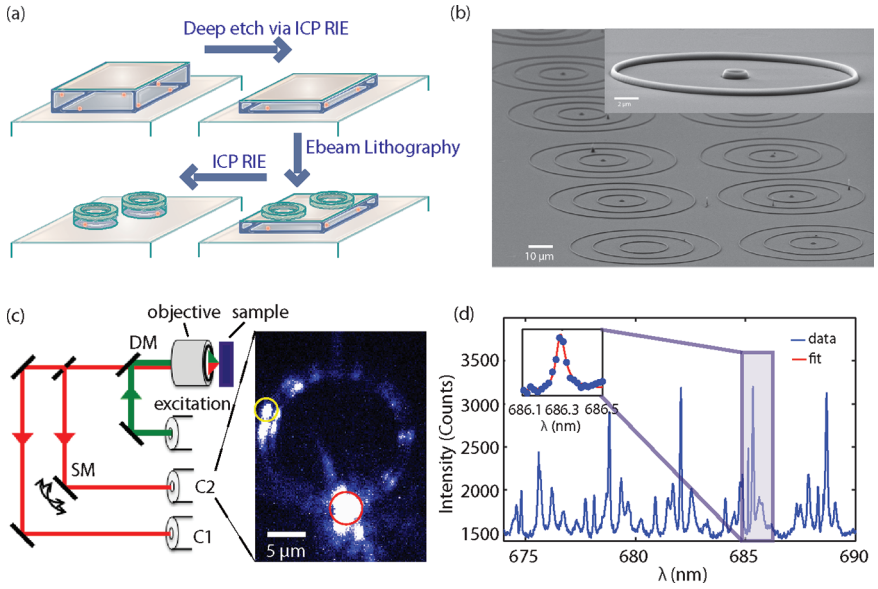


**Figure 1.** (a) Fabrication schematic used to make ring resonators is as follows: First, we thin a diamond slab via an oxygen based reactive ion etch (RIE). Next, we use e-beam lithography to define the devices in e-beam resist. Finally, we transfer the mask into the thinned diamond slab using RIE. Residual resist is not removed from devices during characterization. Optically active defect centers are indicated in red. (b) The SEM image shows diamond ring resonators on SiO2/Si with varying radii. Inset: Higher-magnification image of two ring resonators with smooth sidewalls. (c) Schematic of a two collection arm confocal microscope. Having obtained a scan of the device using collection arm $C_1$ we fix the green pump beam (red circle) and use collection arm $C_2$ to obtain a second scan and collect photons from a different position at the ring resonator (yellow circle). The yellow circle also marks the collection position while taking spectra. (d) The photoluminescence spectrum features peaks that correspond to the modes of the resonator. Inset: A Q-factor of $(12.6 \pm 1) \times 10^3$ is obtained by fitting the experimental data (red).

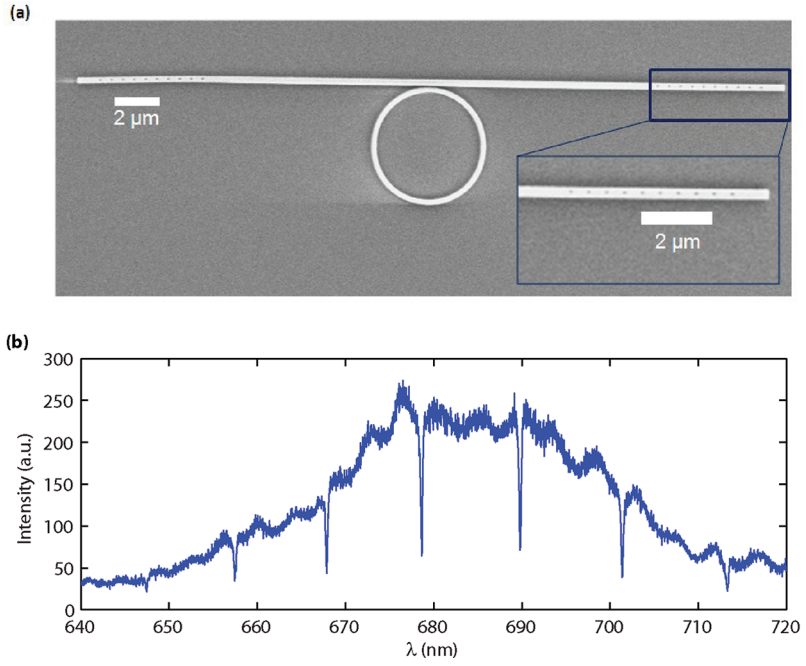


**Figure 2.** (a) SEM image of a single mode ring resonator coupled to a waveguide containing second order gratings on both ends. The ring diameter is 5 $\mu$m and its width is 245 nm. The gap between the waveguide and the ring is 100 nm, while the waveguide itself has a width of 370 nm. The device is sitting on a $SiO_2$/Si substrate. Inset: Magnified image of the grating region. (b) The transmission spectrum is obtained by exciting the structure with white light (from supercontinuum source) using the right-hand side grating and measuring transmitted signal using the left-hand side grating. The dips in the transmission correspond to the ring resonator modes.

mirror, and red photons (650−800 nm) emitted from NV centers are collected and analyzed after passing through a dichroic mirror (DM) and long-pass filters. Our detection path is split into two arms, one of which is always fixed at the excitation spot ($C_1$) while the second arm can be scanned independently ($C_2$). The latter allows us to spatially separate excitation and collection positions. First, we scan the sample to obtain an emission image of the device using $C_1$. Figure 1c (right) shows a scan of the photon collection position over the ring in $C_2$ (yellow circle) while constantly exciting with the


dx.doi.org/10.1021/nl204449n | *Nano Lett.* 2012, 12, 1578−1582

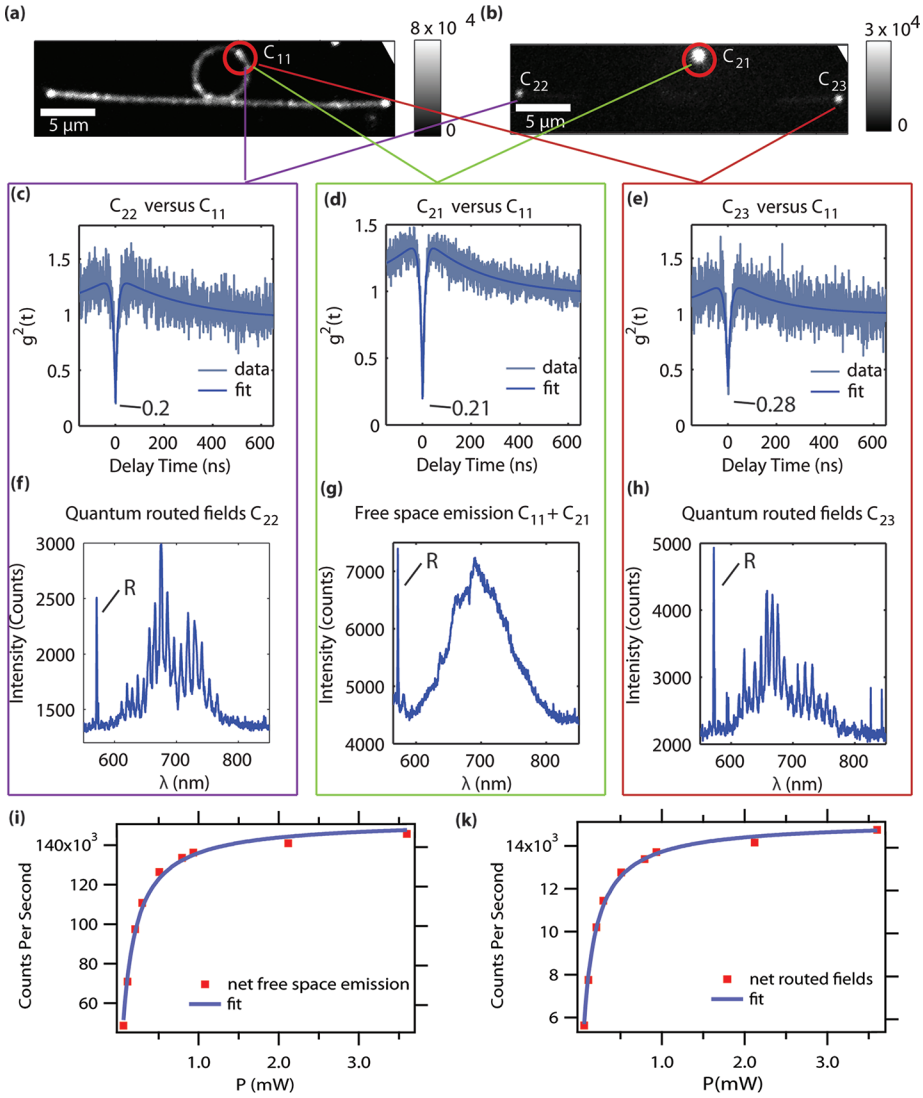


**Figure 3.** (a) Confocal image of the device is obtained by scanning the pump laser and using collection arm $C_1$ to collect the fluorescence (see also Figure 1). After presence of a NV center is confirmed, we position the pump beam at its location. (b) Second confocal image can then be acquired using the collection arm $C_2$. Furthermore, $C_2$ can be used to collect light from three locations of interest: NV center position ($C_{21}$), left-hand side grating ($C_{22}$) and right-hand side grating ($C_{23}$). (c–e) Hanbury–Brown–Twiss apparatus confirms emission and routing of nonclassical light, by cross correlating signals $C_{11}$ with $C_{21}$ as well as $C_{23}$ and $C_{22}$. Strong antibunching ($g^{(2)}(0) < 0.5$) is observed without any background subtraction. (g) The combined spectrum of $C_{11}$ and $C_{21}$ shows the characteristic NV emission. The exact same position of the (nonbroadened) Raman line at 573 nm as in the bulk diamond indicates that the single crystal diamond film quality is comparable to bulk diamond (denoted by *R*). (f,h) Spectra collected from the gratings $C_{22}$, $C_{23}$, respectively, reveal resonances of the ring imprinted on the phonon sideband of the NV center's emission (using a 150 lines/mm grating). We obtain a *Q*-value of $(3.2 \pm 0.4) \times 10^3$ for the resonance at 665.9 nm using a large resolution grating (1800 lines/mm). (i) Free-space collection exhibits a saturated single photon flux of $(15 \pm 0.2) \times 10^4$ CPS at a pump power of $120 \pm 7$ $\mu$W from an NV center. The net counts from a single NV center are obtained via subtracting the linear background from the overall count rate. (k) The combined count rate at both gratings gives a saturation level of $(15 \pm 0.1) \times 10^3$ CPS at a saturation pump power of $(100 \pm 4)$ $\mu$W.

pump laser in the same position (red circle). The device shown in the figure has an outer ring radius of 20 $\mu$m and a 1 $\mu$m × 410 nm cross-section with 300 nm XR covering the diamond. The intensity profile of the ring indicates excitation of a higher order mode (confirmed by 3D finite difference time domain (FDTD) simulations, not shown). The spectrum reveals multimode behavior of the cavity with quality (*Q*) factors of $Q \approx 12\,600$ and a finesse *F* of 62 (Figure 1d and inset).

To form a node of a network it is necessary to integrate the ring resonator with a channel that carries information. We monolithically fabricate ring resonators next to optical waveguides and thereby provide efficient and robust in- and outcoupling of light to the resonator with embedded single NV centers. The waveguides contain second order gratings on each end to facilitate free-space coupling of photons (Figure 2a). We characterize the structure by coupling the light from a broadband white light source into one grating and by collecting transmitted light from the other grating. The transmission spectrum shows regularly spaced dips corresponding to the different (longitudinal) resonant modes of the ring resonator (Figure 2b). We extract a *Q*-factor of $Q \approx 2500$ and $F \approx 40$ for the resonance at $\lambda = 689.8$ nm. Here, we operate close to critical coupling where the decay rate to the waveguide would equal the intrinsic field decay rate of the resonator.

Additionally, we demonstrate efficient generation and routing of nonclassical light fields provided by a single NV center


dx.doi.org/10.1021/nl204449n | *Nano Lett.* 2012, 12, 1578–1582

embedded inside the diamond ring resonator at room temperature. Single photons emitted from the NV center into the ring resonator couple evanescently to the waveguide and are outcoupled one by one by the gratings. Figure 3a,b illustrates scans using the two confocal collection channels $C_1$ and $C_2$, respectively (the device is different from the one shown in Figure 2). We excite an NV center with green light (532 nm) and use collection arm $C_2$ to collect photons from three different locations: directly above the NV center denoted by $C_{21}$, from both grating couplers, $C_{22}$, for the coupler on the left, and $C_{23}$ for the one on the right. Collection arm $C_1$, positioned above the NV center, is used to collect photons emitted directly by the NV center denoted by $C_{11}$. We use Hanbury Brown and Twiss (HBT) configuration[21] to evaluate the second-order intensity correlations $g^{(2)}(\tau)$ where nonclassical light behavior from a single quantum emitter results in $g^{(2)}(0) < 0.5$.[22] First we study the free-space emission of the NV center (Figure 3d). Here, light is directly emitted upward and extracted at the pump position in each collection position ($C_{11}$ and $C_{21}$). The cross-correlation between $C_{11}$ and $C_{21}$ shows strong photon antibunching demonstrating the single photon character of the emitted quantum field. The increased coincidence rate for 12 ns $< \tau <$ 550 ns is attributed to an intermediate shelving state, characteristic of an NV center's emission.[23] When collecting photons emitted directly above the NV center (combining $C_{11}$ and $C_{21}$) we observe the typical NV center's emission spectrum (Figure 3g) where the majority of collected photons are emitted directly into the free-space without coupling into the ring modes. Furthermore, the Raman line occurs at the same spectral position (573 nm) as in bulk diamond, indicating a good film quality (Figure 3, as denoted by $R$ in all spectra). The spectra at the outcoupling gratings (Figure 3f,h) feature prominent peaks indicating coupling of the NV center's fluorescence to the modes of the ring resonator as well as transfer of emitted photons into the waveguide. On the basis of this fluorescence spectrum, we measure loaded $Q$-factors as high as $(3.2 \pm 0.4) \times 10^3$ at 665.9 nm. Moreover, we observe the evidence of routing of the quantum light field when we cross-correlate $C_{11}$ with $C_{22}$ and $C_{23}$. We confirm strong photon antibunching without significant change of the light statistics compared to the autocorrelated free-space emission (Figure 3 panels c amd e, respectively).

Finally, we evaluate the performance of the routing process by comparing the saturation behavior of the NV center emission into free space with its emission into the photonic structure. We obtain the net count rate by subtracting the background (linearly increasing with pump power) from the overall counts and fit according to[23] $I(P) = (I_{Sat})/[1 + (P_{Sat}/P)]$ where $I_{Sat}$ and $P_{Sat}$ are the saturated count intensity and pump power, respectively. The free space emission of the NV center, obtained by adding $C_{11}$ and $C_{21}$, saturates at a count level of $(15 \pm 0.2) \times 10^4$ counts per seconds (CPS) at a pump power of $(120 \pm 7)$ $\mu$W. This saturation level is significantly higher when compared to an NV center in bulk that we attribute to a thin film effect[24] combined with the NV center's polarization-dependent coupling to the ring. At the same time, the combined counts from the outcoupling gratings give $(15 \pm 0.1) \times 10^3$ CPS at saturation at a pump power of $(100 \pm 4)$ $\mu$W. Using 3D FDTD modeling we estimate the overall collection efficiency of our current grating design to be 30%. In addition, by modeling the coupling efficiency from the NV center to the ring and from the ring to the waveguide we estimate a total collection efficiency of our system to be 15%, that is, 15% of photons emitted by an NV center are outcoupled by the gratings and collected using our collection optics. We note that reduced photon counts collected from gratings are largely due to the confocal nature of our experimental apparatus which collects light only from a small (<1 $m^2$) region of the grating. The collection from the gratings could be significantly improved if light from the whole grating regions is collected using a multimode fiber or an objective lens. Improvements in the design of the gratings themselves can increase the collection efficiency up to 90%.[25] Finally, inverse-taper waveguide outcoupling[26,27] could be used to efficiently collect most of the emitted light directly from the waveguide, without a need for a grating.

Our first demonstration of an integrated on-chip optical network based on diamond illustrates the great potential of a diamond-on-insulator platform in the field of quantum optics. The compact architecture and low loss material make our diamond platform suitable for large scale integration where multiple devices can be connected via single photon channels, thus enabling on-chip photonic networks. With the recent progress of spin-photon entanglement with single NV centers,[28] our approach may pave the way for the realization of integrated, scalable quantum networks[4] in which photons are used to transfer quantum information between different nodes (e.g., NV center embedded inside cavity) of the network. Because of their long spin coherence times at room temperature, NV centers are not only promising candidates for quantum memory, but also have intriguing applications in quantum sensing.[19,29,30] In order to enhance the interaction between light and an NV center, and possibly enter the strong-coupling regime of light-matter interaction, photonic crystal cavities fabricated directly in diamond will be explored. Besides other applications, entering the strong coupling regime could be applied to realize single photon transistors[31,32] based on diamond.

## ■ ASSOCIATED CONTENT

### Ⓢ Supporting Information

A more detailed description of the confocal microscope setup containing two collection arms as well as 3D FDTD modeling on the coupling efficiency, mode volume, and Purcell effect of our device. This material is available free of charge via the Internet at http://pubs.acs.org.

## ■ AUTHOR INFORMATION

### Corresponding Author

*E-mail: loncar@seas.harvard.edu.

### Notes

The authors declare no competing financial interest.

## ■ ACKNOWLEDGMENTS

Devices were fabricated in the Center for Nanoscale Systems (CNS) at Harvard. The authors thank Parag Deotare for many helpful discussions and Daniel Twitchen and Matthew Markham from Element Six for support with diamond samples. T.M.B. was supported by the NDSEG and the NSF graduate student fellowships, and J.T.C. by the NSF graduate student fellowship. A.K. acknowledges support from the Alexander von Humboldt Foundation. This work was supported in part by the National Science Foundation (NSF) Nanotechnology and Interdisciplinary Research Team grant (ECCS-0708905), the Defense Advanced Research Projects Agency (Quantum

Entanglement Science and Technology program), and the Hewlett-Packard Foundation as well as AFOSR MURI (Grant FA9550-09-1-0669-DOD35CAP). M.L. acknowledges support from the Sloan Foundation.

## REFERENCES

(1) Wrachtrup, J.; Jelezko, F. *J. Phys.: Condens. Matter* **2006**, *18*, 807–824.
(2) Neumann, P.; Mizuochi, N.; Rempp, F.; Hemmer, P.; Watanabe, H.; Yamasaki, S.; Jacques, V.; Gaebel, T.; Jelezko, F.; Wrachtrup, J. *Science* **2008**, *320*, 1326.
(3) O'Brien, J. L. *Science* **2007**, *318*, 1567.
(4) Kimble, H. J. *Nature* **2008**, *453*, 1023–1030.
(5) Childress, L.; Taylor, J. M.; Sørensen, A. S.; Lukin, M. D. *Phys. Rev. Lett.* **2006**, *96*, 070504.
(6) Beveratos, A.; Brouri, R.; Gacoin, T.; Villing, A.; Poizat, J. P.; Grangier, P. *Phys. Rev. Lett.* **2002**, *89*, 187901.
(7) Aharonovich, I.; Greentree, A. D.; Prawer, S. *Nat. Photonics* **2011**, *5*, 397.
(8) Babinec, T.; Hausmann, B. M.; Khan, M.; Zhang, Y.; Maze, J.; Hemmer, P. R.; Loncar, M. *Nat. Nanotechnol.* **2010**, *5*, 195–199.
(9) Hadden, J. P.; Harrison, J. P.; Stanley-Clarke, A. C.; Marseglia, L.; Ho, Y.-L. D.; Patton, B. R.; O'Brien, J. L.; Rarity, J. G. *Appl. Phys. Lett.* **2010**, *97*, 241901.
(10) Siyushev, P.; Kaiser, F.; Jacques, V.; Gerhardt, I.; Bischof, S.; Fedder, H.; Dodson, J.; Markham, M.; Twitchen, D.; Jelezko, F.; Wrachtrup, J. *Appl. Phys. Lett.* **2010**, *97*, 241902.
(11) Choy, J. T.; Hausmann, B. J. M.; Babinec, T. M.; Bulu, I.; Khan, M.; Maletinsky, P.; Yacoby, A.; Loncar, M. *Nat. Photonics* **2011**, *5*, 738 DOI: 10.1038/nphoton.2011.249.
(12) Barclay, P. E.; Fu, K.-M. C.; Santori, C.; Beausoleil, R. G. *Appl. Phys. Lett.* **2009**, *95*, 191115.
(13) Wang, C. F.; Choi, Y.-S.; Lee, J. C.; Hu, E. L.; Yang, J.; Butler, J. E. *Appl. Phys. Lett.* **2007**, *90*, 081110.
(14) Wang, C. F.; Hanson, R.; Awschalom, D. D.; Hu, E. L. *Appl. Phys. Lett.* **2007**, *91*, 201112.
(15) Hiscocks, M. P.; Ganesan, K.; Gibson, B. C.; Huntington, S. T.; Ladouceur, F.; Prawer, S. *Opt. Express* **2009**, *16* (24), 19512–19519.
(16) Loncar, M.; Babinec, T.; Choy, J.; Hausmann, B.; Bulu, I.; Zhang, Y.; Khan, M.; McCutcheon, M. W. Diamond Nanophotonics and Quantum Optics. In *Artificial Atoms in Diamond: From Quantum Physics to Applications*; Cambridge: New York, 2010.
(17) Hausmann, B.; Choy, J.; Quan, Q.; McCutcheon, M.; Maletinsky, P.; Babinec, T.; Chu, Y.; Kubanek, A.; Yacoby, A.; Lukin, M.; Loncar, M. On-Chip single crystal diamond resonators. In CLEO/QELS 2011, Baltimore, MD, May 1–6, 2011.
(18) Faraon, A.; Barclay, P. E.; Santori, C.; Fu, K.-M. C.; Beausoleil, R. G. *Nat. Photonics* **2010**, *5*, 301–305.
(19) Maletinsky, P.; Hong, S.; Grinolds, M.; Hausmann, B.; Lukin, M. D.; Walsworth, R.-L.; Loncar, M.; Yacoby, A. arXiv:1108.4437.
(20) Akimov, A. V.; Mukherjee, A.; Yu, C. L.; Chang, D. E.; Zibrov, A. S.; Hemmer, P. R.; Park, H.; Lukin, M. D. *Nature* **2007**, *450*, 402–406.
(21) Brown, R. H.; Twiss, R. Q. *Nature* **1956**, *177*, 27–29.
(22) Kimble, H. J.; Dagenais, M.; Mandel, L. *Phys. Rev. Lett.* **1977**, *39*, 691.
(23) Kurtsiefer, C.; Mayer, S.; Zarda, P.; Weinfurter, H. *Phys. Rev. Lett.* **2000**, *85*, 290.
(24) Lee, K. G.; Chen, X. W.; Eghlidi, H.; Kukura, P.; Lettow, R.; Renn, A.; Sandoghdar, V.; Goetzinger, S. *Nat. Photonics* **2011**, *5*, 166.
(25) Laere, F. V.; Roelkens, G.; Ayre, M.; Schrauwen, J.; Taillaert, D.; Thourhout, D. V.; Krauss, T. F.; Baets, R. *J. Lightwave Technol.* **2007**, *25* (1), 151–156.
(26) Almeida, V. R.; Panepucci, R. R.; Lipson, M. *Opt. Lett.* **2003**, *28* (15), 1302–1304.
(27) Shoji, T.; Tsuchizawa, T.; Watanabe, T.; Yamada, K.; Morita, H. *Electron. Lett.* **2002**, *38* (25), 1669–1670.
(28) Togan, E.; Chu, Y.; Trifonov, A. S.; Jiang, L.; Maze, J.; Childress, L.; Dutt, M. V. G.; Sørensen, A. S.; Hemmer, P. R.; Zibrov, A. S.; Lukin, M. D. *Nature* **2010**, *466*, 730–734.
(29) Maze, J. R.; Stanwix, P. L.; Hodges, J. S.; Hong, S.; Taylor, J. M.; Cappellaro, P.; Jiang, L.; Dutt, M. V. G.; Togan, E.; Zibrov, A. S.; Yacoby, A.; Walsworth, R. L.; Lukin, M. D. *Nature* **2008**, *455*, 644.
(30) Balasubramanian, G.; Chan, I. Y.; Kolesov, R.; Al-Hmoud, M.; Tisler, J.; Shin, C.; Kim, C.; Wojcik, A.; Hemmer, P. R.; Krueger, A.; Hanke, T.; Leitenstorfer, A.; Bratschitsch, R.; Jelezko, F.; Wrachtrup, J. *Nature* **2008**, *455*, 648–651.
(31) Chang, D. E.; Sørensen, A. S.; Demler, E. A.; Lukin, M. D. *Nat. Phys.* **2007**, *3*, 807–812.
(32) Hwang, J.; Pototschnig, M.; Lettow, R.; Zumofen, G.; Renna, A.; Götzinger, S.; Sandoghdar, V. *Nature* **2009**, *460*, 76–80.